Title:

Overexpression of TEAD4 in atypical teratoid/rhabdoid tumor: New insight to the pathophysiology of an aggressive brain tumor

Mario Suzuki [1, 2, 3], Akihide Kondo [1], Ikuko Ogino [1], Hajime Arai [1], Tadanori Tomita [2, 4], Simone Treiger Sredni [2, 3, 4]

[1]Department of Neurosurgery, Juntendo University, School of Medicine, Tokyo, Japan; [2]Division of Pediatric Neurosurgery, Ann and Robert H. Lurie Children's Hospital of Chicago; [3]Stanley Manne Children's Research Institute; [4]Northwestern University, Feinberg School of Medicine.

Corresponding author: Mario Suzuki, Department of Neurosurgery, Juntendo University, School of Medicine, 2-1-1 Hongo, Bunkyo-ku, Tokyo 113-8421, Japan.
E-mail: marisuzu@juntendo.ac.jp
Phone: +81-3-3813-3111
Fax: +81-3-5689-8343

Grant sponsor: The Graduate School Research Program from Juntendo University and The Rally Foundation for Childhood Cancer Research in memory of Hailey Trainer;
Grant number: 925540

Conflict of interest: Nothing to declare

Word Count for: a) Abstract: 241 words. b) Main Text: 3423 words.
The manuscript includes: 1 Table, 4 Figures, and 1 Supplementary file.

Short running title: TEAD4 expression in AT/RT

Key words: Atypical teratoid/rhabdoid tumor, AT/RT, Hippo pathway, TEAD4, YAP1

Abbreviations:

AT/RT	Atypical teratoid/rhabdoid tumor
CNV	Copy number variation
CRISPR	Clustered regularly interspaced short palindromic repeats
GE	Gene expression
IHC	Immunohistochemistry
MB	Medulloblastoma
MRT	Malignant rhabdoid tumor
Q-PCR	Quantitative real-time polymerase chain reaction
TEAD4	TEA domain family 4

Abstract

Background: Atypical teratoid/rhabdoid tumor (AT/RT) is a highly malignant embryonal brain tumor that occurs mainly in early childhood. Although most of the tumors are characterized by inactivating mutations of the tumor suppressor gene, *SMARCB1,* the biological basis of its tumorigenesis and aggressiveness is still unknown.

Procedure: We performed high throughput copy number variation analysis of primary cell lines generated from primary and relapsed tumors from one of our patients to identify new genes involved in AT/RT biology. The expression of the identified gene was validated in 29 AT/RT samples by gene expression profiling, Q-PCR, and immunohistochemistry. Furthermore we investigated the function of this gene by mutating it in rhabdoid tumor cells.

Results: *TEAD4* amplification was detected in the primary cell lines and its overexpression was confirmed at mRNA and protein levels in an independent cohort of AT/RT samples. *TEAD4*'s co-activator, *YAP1* and the downstream targets, *MYC* and *CCND1* were also found to be upregulated in AT/RT when compared to medulloblastoma. Immunohistochemistry showed TEAD4 and YAP1 overexpression in all samples. Cell proliferation and migration were significantly reduced in *TEAD4*-mutated cells.

Conclusions: We report the overexpression of TEAD4 in AT/RT, which is a key component of Hippo pathway. Recent reports revealed that dysregulation of the Hippo pathway is implicated in tumorigenesis and poor prognosis of several human cancers. Our results suggest that TEAD4 plays a role in the pathophysiology of AT/RT, which represents a new insight into the biology of this aggressive tumor.

Text

Introduction

Malignant rhabdoid tumor (MRT) is a highly aggressive pediatric embryonal tumor that can arise in any anatomic location. The most frequent sites of origin are the kidneys and the brain.[1] MRT that originates in the central nervous system is called atypical teratoid/rhabdoid tumor (AT/RT). AT/RT comprises approximately 1-2% of all pediatric brain tumors, but it is the most frequent malignant brain tumor among infants.[2, 3] It shows a highly aggressive and unresponsive nature with a median overall survival of 6 to 18 months despite intensive multimodal therapy, including surgery, high-dose chemotherapy with or without intrathecal chemotherapy, and radiation therapy.[4-6] Recently, reports have shown that radiation therapy and intensive multimodal chemotherapy improve the survival of patients especially those older than 3 years of age. However, the prognosis for the majority of patients' population, especially in infants, remains still poor.[6-10]

Histopathologically, AT/RT is characterized by variable amounts of cells with classic rhabdoid phenotype, which shows eccentrically placed nuclei containing vesicular chromatin and abundant cytoplasm with eosinophilic globular inclusions. Usually, these cells with rhabdoid phenotypes are observed within areas of small undifferentiated tumor cells. Therefore, depending on the area examined, it can be misdiagnosed as other embryonal brain tumors such as medulloblastoma (MB) or a group of tumors recognized as the primitive neuroectodermal tumor of the central nervous system (CNS-PNET) in former WHO classification.[11, 12] After the notable discovery of genomic alterations for AT/RT in the *SMARCB1* (*BAF47/hSNF5/INI1*) tumor suppressor gene, which is a component of the chromatin remodeling complex SWItch/Sucrose Non Fermentable (SWI/SNF),[13] negative nuclear stain for SMARCB1 protein has become the widespread procedure for diagnosis of this tumor.[14] While *SMARCB1* mutations are the defining genetic alterations of AT/RT, recent collaborative studies involving large cohorts of samples and advances in genome-wide technologies have suggested the existence of different molecular subgroups.[15-17] Several groups have also explored new potential therapeutic targets.[18-22] Nevertheless, much of the biology contributing to the development and aggressiveness of this tumor is still poorly understood.

TEA domain family member 4 (TEAD4) is a transcriptional factor, which is a part of the Hippo signaling pathway. The Hippo pathway is conserved as a tumor suppressor

pathway and plays a role in several biological processes including organ size control, tissue regeneration, cancer development, stem cell self-renewal and differentiation.[23, 24] The pathway consists of two serine/threonine kinases MST and LAT, the transcriptional co-activators YAP1 and TAZ, and the transcription factors TEAD1 to TEAD4. When the Hippo pathway is activated, the activity of YAP1 is inhibited and the expression of its downstream genes is suppressed. Conversely, when the pathway is inactivated, YAP1 accumulates in the nucleus and form complexes with TEADs and other transcription factors, promoting cell proliferation and cell survival and inhibiting apoptosis.[25] Recently, several studies have found that mutations and altered expression of a subset of Hippo signaling pathway genes are involved in increased cell proliferation in diverse types of human cancers such as melanoma, ovarian, breast, gastric and colorectal cancers. Some of these reports suggest that the dysregulation of this pathway correlates with poorer prognosis.[24, 26-29]

To clarify the aggressiveness of this tumor we performed genome-wide studies in samples from our patients including primary and relapsed tumors after interventions and found the amplification of *TEAD4*. Then, we validated the overexpression at both mRNA and protein levels in a larger set of samples. Its transcriptional co-activator YAP1 and downstream targets were also found to be upregulated in AT/RT, which may indicate the active status of TEAD4. Furthermore, we detected decrease in cell proliferation and migration in a *TEAD4*-mutated rhabdoid tumor cell line. Those facts suggest that this pathway may have a key role on this tumor's biology.

Materials and Methods

Tumor samples

Tumor samples, including fresh frozen tumor tissues and formalin-fixed and paraffin-embedded (FFPE) tissue sections, were collected from patients diagnosed with AT/RT and MB. The diagnoses were confirmed pathologically according to the current WHO criteria.[11, 12] Tumors were provided by the Juntendo University Hospital (Tokyo, Japan), the Falk Brain Tumor Bank (Chicago, IL, USA), and the Center for Childhood Cancer, Biopathology Center (Columbus, OH, USA), which is a section of Cooperative Human Tissue Network of The National Cancer Institute (Bethesda, MD, USA). Written informed parental consents were obtained prior to sample collection. This study was approved by the institutional review boards of Juntendo University (IRB#2010-014) and

Ann and Robert H. Lurie Children's Hospital of Chicago (IRB#2009-13778). Primary AT/RT samples from 29 patients, 4 samples from relapsed tumor tissues (Table 1) and 15 medulloblastomas were included in our studies.

Primary cell culture

Primary AT/RT cell lines were established from the primary and relapsed tumors from one of our patients. Tumor tissues were obtained at surgery, and minced in a petri dish, and then maintained in Neurobasal-A Medium with 2% B-27 Supplement serum free, EGF, FGF-Basic, and Penicillin-Streptomycin-Glutamine (Thermo Fisher Scientific, USA) at 37ºC, 5% CO_2.[30] Cellblocks were made using Array Jelly (Youken-Science Co., Ltd, Japan) according to the manufacture's protocol.

Copy Number Variations (CNVs)

Genomic DNA was isolated from both primary cell lines as described above and from the correspondent relapsed tissue using Gentra Purgene Tissue Kit (Qiagen, Germany) according to the manufacture's protocol.

A total of 250 ng of genomic DNA was used to investigate genomic alterations using the Genome-Wide Human CytoScan HD Array (Affymetrix, USA) according to the manufacture's protocol. The data was analyzed with Affymetrix® Chromosome Analysis Suite v1.2 (Affymetrix Inc., USA).

In situ hybridization

In situ hybridization was performed on FFPE sections of the primary and relapse samples from which the primary cell lines were established, using GeneticLab QuantiGene ViewRNA kit (Affymetrix, USA). After deparaffinization, sections were boiled in pretreatment solution for 20 minutes, digested with protease for 20 minutes, and then hybridized with designed probes against *TEAD4* (VX1-99999-01) and *YAP1* (VX6-99999-01). Fast Blue and Fast Red substrates were used to produce signals.

Gene expression (GE) profiling

Total RNA was isolated using Trizol Reagent (Invitrogen, USA) from frozen tumor tissues.

GE profiling was performed using Illumina HT-12 BeadChip whole-genome expression

arrays (Illumina, USA). All RNA samples were treated with DNase. *In vitro* transcription was completed in order to synthesize biotin-labeled cDNA. A total of 1.5 µg of cDNA was hybridized to each array using standard Illumina protocols. Slides were scanned and analyzed using BeadStudio (Illumina, USA). Data was normalized using the quantile normalization procedure from the bioconductor package, *affy* (www.bioconductor.org). Kyoto Encyclopedia of Genes and Genomes – KEGG (http://www.kegg.jp/kegg/) was referred to identify enriched biological functions.

Quantitative real-time PCR (Q-PCR)

A total of 1000 ng of RNA was used to make cDNA using the high capacity RNA-to-cDNA Kit (Life Technologies, USA). The expression of selected genes was validated by TaqMan gene expression assays (Life Technologies, USA). The following genes were tested: *TEAD4* (Hs01125032_m1), *YAP1* (Hs00902712_g1), *MYC* (Hs00153408_m1), and *CCND1* (Hs0076553_m1). The normalized expression levels were calculated by the ΔΔCt method using the housekeeping gene *GAPDH* (Hs02758991_g1) as a reference.

Q-PCR for CNVs was performed using TaqMan Copy Number Assays (Life Technologies, USA) according to the manufacture's protocol. Three *TEAD4* probes were tested (Hs01275079_cn, Hs00784753_cn, and Hs01667625_cn) and RNase P was used as a reference. The data was analyzed with Copy Caller Software (Applied Biosystem, USA).

Immunohistochemistry (IHC)

FFPE tumor tissue sections were stained using standard immunohistochemical methods with the following antibodies: polyclonal hSNF5 antibody (1:200 Novus Biologicals, USA), polyclonal TEAD4 antibody (1:200 Abcam, UK), monoclonal YAP1 antibody (1:200 Abnova, Taiwan), polyclonal Ki-67 antibody (1:200 Thermo Scientific, USA), and polyclonal Phospho-Histone H3 antibody (PHH3) (1:5,000 Abcam, UK). Slide interpretation was performed independently by two investigators in a blinded fashion (MS and STS).

Western Blotting

After cells were lysate, protein concentration was calculated using Pierce BCA Protein

Assay Kit (Thermo Fisher Scientific, USA). A total of 20 µg of proteins were loaded onto a SDS gel and transferred to a PVDF membrane. The following antibodies were used for protein detection: monoclonal TEAD4 antibody (1:1,000 Abcam, UK) and monoclonal GAPDH loading control antibody (1:25,000 Thermo Fisher Scientific, USA). Protein levels were detected by ECL detection solution (Thermo Fisher Scientific, USA) and visualized on Bio-Rad ChemiDoc MP (Bio-Rad, USA).

In vitro genome edition

We used Lentiviral-CRISPR/Cas9 system to mutate *TEAD4* in the MON cell line. MON cell line, which was a gift from Dr. Delattre (Institute Curie, France), was established from a human malignant rhabdoid tumor (MRT) of soft tissue.[31, 32] Prior to the genome edition, *TEAD4* copy number amplification in MON cell line was confirmed by Q-PCR (Fig. 3A). The cells were maintained in HyClone RPMI 1640 (Thermo Fisher Scientific, USA) with 10% of FBS and penicillin/streptomycin at 37ºC, 5% CO_2.

Lentiviral-CRISPR/Cas9 particles (Sigma-Aldrich, USA) were used for targeted genome editing. gRNA for HPRT was used as a positive control, and scrambled gRNA was used as a negative control. After transduction, cells were selected with puromycin for 14 days. The transduction efficiencies were confirmed with GeneArt Genomic Cleavage Detection kit (Life technologies, USA) in order to detect the locus-specific double-strand break formation and to verify the efficiency of the genome edition.

Cell proliferation assay

Cellular proliferation was assessed by TACS MTT Cell Proliferation Assays (Trevigen, USA) according to the manufacture's protocol. Absorbance was measured at 540 nm using a microplate reader after 24, 48, 72, and 96 hours. Each experiment was performed in triplicate. We also evaluated cell proliferative activity by IHC. Positive cells for Ki-67 and PHH3 were counted in five fields with 40X magnification in both wild type MON cells (WT) and *TEAD4*-mutated MON cells (*TEAD4*-mut).

Cell migration assay

Cell migration was assessed using a 24-well Transwell chamber system (Corning, USA).[33] After 24 hours of incubation, the cells were fixed with formalin, stained by cresyl violet, and counted using an inverted microscope. Each experiment was

performed in triplicate.

Results

Tumor samples and primary cell cultures

Primary AT/RT samples from 29 patients (the median age at diagnosis was 3-year-old with range from 2-month-old to 13-year-old, M: F = 13: 7) and additional 4 samples from corresponding relapsed tumor tissues were included in this study as described in Table 1~~I~~. Fifteen MB samples were included in the study (the mean age at diagnosis was 5-years-old with range from 0-year-old to 10-year-old, M: F = 10: 5).

Primary cell lines were established from tumors of patient number 1, who was a six month old girl having a tumor in the posterior fossa. Two months after near total removal, the tumor relapsed during the course of high dose chemotherapy. Radiation therapy was performed after the second surgery, but the patient died of disease progression six months after her admission. From the first and second surgeries, primary cell lines were established. Hematoxylin and eosin (H & E) stained slides revealed extensive areas of small undifferentiated cells and focal fields of rhabdoid cells (Figs. 1A, D, G, and J). In regards to the primary cell lines, the morphological features observed on cell block sections were consistent with the histology of the original tumor tissue sections. The diagnoses of AT/RT were further corroborated by loss of SMARCB1 nuclear expression in tumor cells with the presence of an appropriate internal positive control (Figs. 1C and I). Both sections of cell blocks from established cell lines also showed loss of SMARCB1 nuclear expression (Figs. 1F and L). High proliferative activity as detected by IHC for Ki-67 was also demonstrated in all AT/RT samples and cell lines (Figs. 1B, E, H, and K).

TEAD4 and *YAP1* overexpression in primary cell lines

CNVs were analyzed in the two primary cell lines, generated from primary and relapsed tumors, and in the correspondent relapsed tumor tissue. The chromosomal regions showing amplifications or deletions with more than two-fold difference were selected. A total of 31 amplification sites and three deletion sites were detected. Three genes including *TEAD4* were amplified within all the samples (~~Supplementary~~ Supplemental Table S1~~I~~).

Then, the mRNA levels of *TEAD4* and its co-activator *YAP1* were investigated by *In*

situ hybridization. Both primary and relapsed tumor tissues had significantly higher expression of *TEAD4* and *YAP1* when compared to normal brain tissue, but no differences between primary and relapsed tumors were observed ($P = 0.0055$ and $P < 0.0001$ respectively, one-way ANOVA) (Fig. 2A).

Verification of TEAD4 and YAP1 overexpression in an independent set of samples

To verify the TEAD4 and YAP1 overexpression, GE profiling was evaluated in an independent set of 24 AT/RT and 15 MB samples. The expression of both *TEAD4* and *YAP1* was significantly higher in AT/RT (Fold changes = 1.95 and 5.56 respectively. $P < 0.0001$, Mann-Whitney test) (Fig. 2B). The correlation between expression levels and molecular subgroups as defined by Torchia *et al.*[16] and by Johann *et al.*[17] was investigated. *TEAD4* expression in Torchia's group 1 was significantly lower than in group 2 ($P < 0.0001$). Johann's ATRT-SHH, showed a tendency to express *TEAD4* in lower levels when compared to ATRT-TYR and ATRT-MYC. *YAP1* was also less expressed in Torchia's group 1 and in Johann's ATRT-SHH. The expression levels of both *TEAD4* and *YAP1* did not show correlation with age, gender, or tumor location.

The expression levels of all components of the Hippo signaling pathway according to KEGG were investigated. *MST* and *LATS*, upstream kinases of the pathway, did not show differences in expression between AT/RT and MB. The expression of *MER*, *KIBRA*, and *FRMD*, which are considered to be regulators of these kinases even though their function in the Hippo pathway has not been revealed yet, also did not show differential expression. The downstream targets of the Hippo pathway, *MYC* and *CCND1* were significantly overexpressed in AT/RT (Fold changes = 3.56 and 15.7, $P = 0.0001$ and $P < 0.0001$ respectively, Mann-Whitney test) (Fig. 2B). GE profiling was validated by Q-PCR in 8 AT/RT and 6 MB samples (Fold changes = 1.95, 5.56, 3.56, and 15.7, $P = 0.0007$, 0.0007, 0.0027, and 0.0047 respectively, Mann-Whitney test) (Fig. 2C).

The protein expression of TEAD4 and YAP1 was investigated by IHC in 16 FFPE samples of 12 patients (Table 1). All sections including primary and relapsed tumor tissues, showed high expression of both TEAD4 and YAP1. TEAD4 was expressed almost exclusively in the nuclei, while YAP1 expression was observed both in the cytoplasm and the nuclei of tumor cells. Neither the intensity of expression nor the localization of both proteins differed between primary and relapsed tumors (Fig. 2D).

TEAD4-mutated MRT cell line by CRISPR/Cas9

We used Lentiviral-CRISPR/Cas9 system to mutate *TEAD4* in the MON cell line. Transfection efficacy was estimated by the percentage of GFP positive cells (Fig. 3B) and genome edition was confirmed by GCD assay (Fig. 3C). The result from Q-PCR showed 42% reduction of mRNA level of *TEAD4* in mutated cells, and protein level was evaluated by western blotting (Fig. 3D).

Decreased cell proliferation and migration in *TEAD4*-mutated MRT cells

Cellular proliferation was assessed by MTT assay and IHC for Ki-67 and PHH3 antibodies. MTT assay showed statistically significant decrease in cell proliferation in *TEAD4*-mut when compared with WT at all time points (P = 0.0020, 0.0021, 0.0025, and 0.0193 respectively, unpaired t-test) (Fig. 4A). IHC for Ki-67 showed high proliferation in both cell lines. However, there were significantly less Ki67 positive cells within *TEAD4*-mut than within WT ($P = 0.0021$, unpaired t-test) (Fig. 4B). Mitotic activity, measured by PHH3 antibody, was also significantly lower in the *TEAD4*-mut ($P = 0.0147$, unpaired t-test) (Fig. 4C). Notably, cellular migration was significantly inhibited in *TEAD4*-mut when compared with WT ($P < 0.0001$, unpaired t-test) (Fig. 4D).

Discussion

In this study, we report our finding of copy number amplification of *TEAD4* and explore the overexpression of TEAD4 and YAP1 in AT/RT. TEAD4 and YAP1 are key components of Hippo signaling pathway, which has been recognized as a tumor suppressor pathway in recent years.[23, 34-36] We revealed the copy number amplification of *TEAD4* in primary cell lines and correspondent relapsed tissue from a patient. Then, we confirmed the overexpression of TEAD4 and its co-activator YAP1 at mRNA level and at protein level in the same patient's samples. Finally, we validated our findings in an independent cohort of samples. To the best of our best knowledge, this is the first time TEAD4 overexpression is reported in AT/RT.

In normal cells, polarity and adhesion complexes regulate the Hippo pathway and the pathway controls organ size and regeneration through the inhibition of cell proliferation and promotion of apoptosis.[37-39] While, in several human cancers, this pathway is

dysregulated and this dysregulation is supposed to contribute to cancer development. Though many publications report upregulation of *YAP1*, only a few reports describe upregulation of *TEAD4* in cancer.[24, 26, 29] Liu *et al*. reported that, in colorectal cancer, increased TEAD4 expression is a result of copy number amplification.[29] We also observed copy number amplification and overexpression at mRNA and protein levels of TEAD4 in AT/RT.

Since YAP1 cannot bind to DNA by itself, the YAP1 protein in the nuclei is required to be co-localized with TEAD4 for the oncogenic activation of YAP1.[23] The co-localization of TEAD4 and YAP1 in nuclei has been correlated with poor prognosis in human malignancies such as ovarian cancer and gastric cancer.[24, 26] In this study we compared AT/RT to MB, which is the most common pediatric embryonal tumor in the CNS and has a better outcome than AT/RT, with over 90% of cure rates for WNT group and 40-60% for Group 3.[40, 41] Due to the insufficient clinical information, we could not analyze the correlation between the expression levels and the clinical outcome in our AT/RT cohort.

Lim *et al*. reported that the knockdown of *TEAD4* resulted in the reduced growth of gastric cancer cells *in vitro* and *in vivo*.[24] In this study we knocked down *TEAD4* in the MON cell line, which is a well-characterized MRT cell line, and we observed both decrease in proliferation and inhibition of migration of *TEAD4* mutated rhabdoid cells. Although our results are in accordance with the literature, we appreciate the fact that the use of MON may be somehow controversial. While some authors suggested that the differences between MRTs arising in different locations are minimal,[1] other investigator demonstrated low overlap in gene expression of AT/RT and RTK.[42] Knocking down *TEAD4* in AT/RT cell line may clarify this question.

Based on these findings, we suggest that TEAD4, together with its co-activator YAP1 functions as oncogenes and may contribute to the biology of AT/RT.

Overexpression of *MYC* and *CCND1* has been extensively reported in AT/RT.[43, 44] They are already well known proto-oncogenes and also downstream targets of the Hippo pathway. On the other hand, both *MYC* and *CCND1* are part of the Wnt pathway that is known to be dysregulated in a subset of AT/RT.[45] Recently, Johann *et al*. proposed the existence of three AT/RT epigenetic subgroups: ATRT-TYR, ATRT-SHH, and ATRT-MYC. Each of these groups has different clinical characteristics and subgroup-specific networks, granting the possibility of therapeutic intervention.[17] *MYC*

overexpression is the marker of ATRT-MYC and *CCND1* was proposed to be the specific enhancer for ATRT-TYR subgroup. Neither *TEAD4* nor *YAP1* are included in the genetic signatures or networks proposed by the authors. We used their classification system to categorize our 24 AT/RT samples, and observed that ATRT-SHH has a tendency to express *TEAD4* and *YAP1* at lower levels. Another molecular classification was proposed by Torchia *et al.* taking into consideration anatomical location, clinical features, and the level of *ASCL1*, a gene involved in the Notch signaling pathway.[16] We observed that Group 1 AT/RT, that is ASCL1-positive, had significantly lower expression of *TEAD4* when compared to group 2. No difference in *YAP1* was observed.[46] *CCND1* was overexpressed in all our samples. We cannot affirm, based on our results, that overexpression of *MYC* and *CCND1* is a direct response of *TEAD4* activation, as no other component of the pathway was found to be differentially expressed in our samples. Furthermore, it is supposed that other cancer related pathways such as TGF-β signaling pathway and Wnt signaling pathway also regulate the downstream targets of the Hippo pathway. Further studies are needed to investigate the effects of *TEAD4* activation on the Hippo pathway in AT/RT.

In conclusion, we report the overexpression of TEAD4 in AT/RT. High TEAD4 expression was observed in all our cases, including primary and relapsed tumors, at both mRNA and protein levels. Moreover our results showed that TEAD4 knock down significantly impaired proliferative activity *in vitro*. It is feasible to therapeutically target AT/RT by inhibiting the interaction between YAP1 and TEAD4 as has been done in other human cancers.[35] Although TEAD4 may be an essential component of AT/RT biology, further studies are needed to explore the functional significance of these findings and whether the Hippo pathway is an essential component of AT/RT biology.

Acknowledgements

This work was supported by Graduate School Research Program from Juntendo University, Juntendo University Research Institute for Disease of Old Ages, and the Rally Foundation for Childhood Cancer Research in memory of Hailey Trainer.

We thank Miyuki Kunichika, Naira Margarian DVM, PhD, Lin Li MD, MSc, and Dorina Veliceasa PhD for technical assistance and Jessica Jacubowski BSc for editorial support. We also thank all the patients, their families, and the people who work for our patients.

References

1. Grupenmacher AT, Halpern AL, Bonaldo Mde F, et al., Study of the gene expression and microRNA expression profiles of malignant rhabdoid tumors originated in the brain (AT/RT) and in the kidney (RTK). Childs Nerv Syst 2013; 29: 1977-83.
2. Woehrer A, Slavc I, Waldhoer T, et al., Incidence of atypical teratoid/rhabdoid tumors in children: a population-based study by the Austrian Brain Tumor Registry, 1996-2006. Cancer 2010; 116: 5725-32.
3. Ginn KF, Gajjar A, Atypical teratoid rhabdoid tumor: current therapy and future directions. Front Oncol 2012; 2: 114.
4. Athale UH, Duckworth J, Odame I, Barr R, Childhood atypical teratoid rhabdoid tumor of the central nervous system: a meta-analysis of observational studies. J Pediatr Hematol Oncol 2009; 31: 651-63.
5. von Hoff K, Hinkes B, Dannenmann-Stern E, et al., Frequency, risk-factors and survival of children with atypical teratoid rhabdoid tumors (AT/RT) of the CNS diagnosed between 1988 and 2004, and registered to the German HIT database. Pediatr Blood Cancer 2011; 57: 978-85.
6. Benesch M, Bartelheim K, Fleischhack G, et al., High-dose chemotherapy (HDCT) with auto-SCT in children with atypical teratoid/rhabdoid tumors (AT/RT): a report from the European Rhabdoid Registry (EU-RHAB). Bone Marrow Transplant 2014; 49: 370-5.
7. Lafay-Cousin L, Hawkins C, Carret AS, et al., Central nervous system atypical teratoid rhabdoid tumours: the Canadian Paediatric Brain Tumour Consortium experience. Eur J Cancer 2012; 48: 353-9.
8. Slavc I, Chocholous M, Leiss U, et al., Atypical teratoid rhabdoid tumor: improved long-term survival with an intensive multimodal therapy and delayed radiotherapy. The Medical University of Vienna Experience 1992-2012. Cancer Med 2014; 3: 91-100.
9. Zaky W, Dhall G, Ji L, et al., Intensive induction chemotherapy

followed by myeloablative chemotherapy with autologous hematopoietic progenitor cell rescue for young children newly-diagnosed with central nervous system atypical teratoid/rhabdoid tumors: the Head Start III experience. Pediatr Blood Cancer 2014; 61: 95-101.

10. DiPatri AJ, Jr., Sredni ST, Grahovac G, Tomita T, Atypical teratoid rhabdoid tumors of the posterior fossa in children. Childs Nerv Syst 2015; 31: 1717-28.
11. Louis DN, Ohgaki H, wiestler OD, Cavenee WK, WHO Classification of Tumours of the Central Nervous System, Fourth Edition. 2007.
12. Louis DN, Perry A, Reifenberger G, et al., The 2016 World Health Organization Classification of Tumors of the Central Nervous System: a summary. Acta Neuropathol 2016; 131: 803-20.
13. Biegel JA, Zhou JY, Rorke LB, et al., Germ-line and acquired mutations of INI1 in atypical teratoid and rhabdoid tumors. Cancer Res 1999; 59: 74-9.
14. Judkins AR, Mauger J, Ht A, Rorke LB, Biegel JA, Immunohistochemical analysis of hSNF5/INI1 in pediatric CNS neoplasms. Am J Surg Pathol 2004; 28: 644-50.
15. Birks DK, Donson AM, Patel PR, et al., High expression of BMP pathway genes distinguishes a subset of atypical teratoid/rhabdoid tumors associated with shorter survival. Neuro Oncol 2011; 13: 1296-307.
16. Torchia J, Picard D, Lafay-Cousin L, et al., Molecular subgroups of atypical teratoid rhabdoid tumours in children: an integrated genomic and clinicopathological analysis. Lancet Oncol 2015; 16: 569-82.
17. Johann PD, Erkek S, Zapatka M, et al., Atypical Teratoid/Rhabdoid Tumors Are Comprised of Three Epigenetic Subgroups with Distinct Enhancer Landscapes. Cancer Cell 2016; 29: 379-93.
18. Lee S, Cimica V, Ramachandra N, Zagzag D, Kalpana GV, Aurora A is a repressed effector target of the chromatin remodeling protein INI1/hSNF5 required for rhabdoid tumor cell survival. Cancer Res 2011; 71: 3225-35.

19. Smith ME, Cimica V, Chinni S, et al., Therapeutically targeting cyclin D1 in primary tumors arising from loss of Ini1. Proc Natl Acad Sci U S A 2011; 108: 319-24.
20. Alimova I, Birks DK, Harris PS, et al., Inhibition of EZH2 suppresses self-renewal and induces radiation sensitivity in atypical rhabdoid teratoid tumor cells. Neuro Oncol 2013; 15: 149-60.
21. Sredni ST, Patel K, D'Almeida Costa F, de Fatima Bonaldo M, Tomita T, Activation of ErbB2- ErbB3 signaling pathway supports potential therapeutic activity of ErbB inhibitors in AT/RT. J Neurooncol 2014; 118: 201-3.
22. Fruhwald MC, Biegel JA, Bourdeaut F, Roberts CW, Chi SN, Atypical teratoid/rhabdoid tumors-current concepts, advances in biology, and potential future therapies. Neuro Oncol 2016.
23. Nishio M, Otsubo K, Maehama T, Mimori K, Suzuki A, Capturing the mammalian Hippo: elucidating its role in cancer. Cancer Sci 2013; 104: 1271-7.
24. Lim B, Park JL, Kim HJ, et al., Integrative genomics analysis reveals the multilevel dysregulation and oncogenic characteristics of TEAD4 in gastric cancer. Carcinogenesis 2014; 35: 1020-7.
25. Johnson R, Halder G, The two faces of Hippo: targeting the Hippo pathway for regenerative medicine and cancer treatment. NATURE REVIEWS 2014; 13: 63-79.
26. Xia Y, Chang T, Wang Y, et al., YAP promotes ovarian cancer cell tumorigenesis and is indicative of a poor prognosis for ovarian cancer patients. PLoS One 2014; 9: e91770.
27. Yuan H, Liu H, Liu Z, et al., Genetic variants in Hippo pathway genes YAP1, TEAD1 and TEAD4 are associated with melanoma-specific survival. Int J Cancer 2015; 137: 638-45.
28. Wang C, Nie Z, Zhou Z, et al., The interplay between TEAD4 and KLF5 promotes breast cancer partially through inhibiting the transcription of p27Kip1. Oncotarget 2015; 6: 17685-97.
29. Liu Y, Wang G, Yang Y, et al., Increased TEAD4 expression and nuclear localization in colorectal cancer promote

epithelial-mesenchymal transition and metastasis in a YAP-independent manner. Oncogene 2015.

30. Xu J, Erdreich-Epstein A, Gonzalez-Gomez I, et al., Novel cell lines established from pediatric brain tumors. J Neurooncol 2012; 107: 269-80.
31. Zhang ZK, Davies KP, Allen J, et al., Cell cycle arrest and repression of cyclin D1 transcription by INI1/hSNF5. Mol Cell Biol 2002; 22: 5975-88.
32. Versteege I, Medjkane S, Rouillard D, Delattre O, A key role of the hSNF5/INI1 tumour suppressor in the control of the G1-S transition of the cell cycle. Oncogene 2002; 21: 6403-12.
33. Zheng B, Liang L, Huang S, et al., MicroRNA-409 suppresses tumour cell invasion and metastasis by directly targeting radixin in gastric cancers. Oncogene 2012; 31: 4509-16.
34. Lamar JM, Stern P, Liu H, et al., The Hippo pathway target, YAP, promotes metastasis through its TEAD-interaction domain. Proc Natl Acad Sci U S A 2012; 109: E2441-50.
35. Johnson R, Halder G, The two faces of Hippo: targeting the Hippo pathway for regenerative medicine and cancer treatment. Nat Rev Drug Discov 2014; 13: 63-79.
36. Chan SW, Lim CJ, Chen L, et al., The Hippo pathway in biological control and cancer development. J Cell Physiol 2011; 226: 928-39.
37. Ota M, Sasaki H, Mammalian Tead proteins regulate cell proliferation and contact inhibition as transcriptional mediators of Hippo signaling. Development 2008; 135: 4059-69.
38. Zhao B, Tumaneng K, Guan KL, The Hippo pathway in organ size control, tissue regeneration and stem cell self-renewal. Nat Cell Biol 2011; 13: 877-83.
39. Zhou Y, Huang T, Cheng AS, et al., The TEAD Family and Its Oncogenic Role in Promoting Tumorigenesis. Int J Mol Sci 2016; 17.
40. Massimino M, Biassoni V, Gandola L, et al., Childhood medulloblastoma. Crit Rev Oncol Hematol 2016; 105: 35-51.
41. Coluccia D, Figuereido C, Isik S, Smith C, Rutka JT,

Medulloblastoma: Tumor Biology and Relevance to Treatment and Prognosis Paradigm. Curr Neurol Neurosci Rep 2016; 16: 43.

42. Birks DK, Donson AM, Patel PR, et al., Pediatric rhabdoid tumors of kidney and brain show many differences in gene expression but share dysregulation of cell cycle and epigenetic effector genes. Pediatr Blood Cancer 2013; 60: 1095-102.
43. Fujisawa H, Misaki K, Takabatake Y, Hasegawa M, Yamashita J, Cyclin D1 is overexpressed in atypical teratoid/rhabdoid tumor with hSNF5/INI1 gene inactivation. J Neurooncol 2005; 73: 117-24.
44. Hanahan D, Weinberg RA, The hallmarks of cancer. Cell 2000; 100: 57-70.
45. Chakravadhanula M, Hampton CN, Chodavadia P, et al., Wnt pathway in atypical teratoid rhabdoid tumors. Neuro Oncol 2015; 17: 526-35.
46. Fernandez LA, Northcott PA, Dalton J, et al., YAP1 is amplified and up-regulated in hedgehog-associated medulloblastomas and mediates Sonic hedgehog-driven neural precursor proliferation. Genes Dev 2009; 23: 2729-41.

Figure legends:

Figure 1: Establishment of primary cell cultures derived from primary and relapsed tumor tissue. (A, G) H&E staining revealed the presence of small undifferentiated cells and focal fields of rhabdoid cells in primary and relapsed tumor tissues. Characteristic rhabdoid cells were observed in inserts. **(B, H)** High percentage for Ki-67 positive cells (>50%) is observed in both primary and relapse tumors. **(C, I)** Nuclear immunostaining of SMARCB1 (BAF47/hSNF5/INI-1) was absent. Positive internal control was demonstrated in the inserts. **(D, J)** H&E staining of cultured cells revealed the presence of small undifferentiated cells and focal fields of rhabdoid cells demonstrating that cultured cells have similar morphology of the corresponding primary tumor tissues. **(E, K)** High proliferative status of cultured cells as demonstrated by positive Ki-67 immunostaining (>50%). **(F, L)** Nuclear immunostaining of SMARCB1 was absent in both primary and relapsed tissue derived cells. Normal kidney tissue was stained at the same time as a positive control for SMARCB1 (Upper right) (all images: 40x, inserts: 160x digital).

Figure 2: Overexpression of TEAD4 and YAP1 in AT/RT. (A) *In situ hybridization* for *TEAD4* and *YAP1* on samples from patient number 1. The results were analyzed by counting existing dots of mRNA and comparing tumor cells to surrounding normal cells. *TEAD4* and *YAP1* showed significantly higher expression in tumors, for both primary and relapse when compared with normal cerebellum ($P = 0.0055$ and $P < 0.0001$ respectively, one-way ANOVA). **(B)** Gene expression analysis showed significantly higher expression of *TEAD4*, *YAP1*, *MYC*, and *CCND1* in AT/RT when compared to MB (Fold changes = 1.95, 5.56, 3.56, and 15.7 respectively. ****$P < 0.0001$ and ***$P = 0.0001$, Mann-Whitney test). **(C)** Microarray gene expression data was validated by quantitative real-time PCR. All of above genes were significantly overexpressed in AT/RT (Fold changes = 8.62, 17.2, 7.91, and 16.2 respectively. ***$P < 0.001$ and **$P < 0.01$, Mann-Whitney test). **(D)** Immunohistochemistry for TEAD4 and YAP1 from samples of patient number 1 (40x; insert 160x digital). TEAD4 and YAP1 were highly expressed in AT/RT both primary and relapsed tumor tissues. TEAD4 was localized in nuclei and YAP1 was localized in both cytoplasm and nuclei.

Figure 3: *TEAD4*-mutated MRT cell line. (A) Copy number amplification of *TEAD4* is observed in MON cell line. Normal blood cells were used as control. **(B)** Post-transduced images (10x, Right; bright field, Left; fluorescent microscope). GFP-positive cells indicated the efficiency of transduction: 22.3%. **(C)** GCD assay showed two cleaved bands below the parental band in *TEAD4*-mutated cells, confirming genome editing. Two sets of primers were designed as follows: primer 1; 3'-TGTGATCCAGAGAGGGAACC and 5'-CATTGAACCCAGGAGGAGA, primer 2; 3'-TGTGATCCAGAGAGGGAACC and 5'-TCACTTGAACCCAGGAGGAG. **(D)** Q-PCR shows 42% reduction of *TEAD4* expression in mutated cells and western blotting demonstrates that TEAD4 expression was suppressed in mutated cells despite the equal level of endogenous control, GAPDH.

Figure 4: Cell proliferation was decreased in *TEAD4*-mutated MRT cell line. (A) MTT proliferation assay: significantly lower cell proliferation was observed in *TEAD4*-mutated cells when compared to wild type (unpaired t-test; $*P < 0.05$, $**P < 0.005$). **(B)** Representative images and analysis of Ki-67 (40x): positive percentage was significantly higher in wild type (unpaired t-test; $**P < 0.005$). **(C)** Representative images and analysis of PHH3 antibody (40x): mitotic activity was detected by PHH3 staining. *TEAD4*-mutated cells showed significantly lower mitotic activity (unpaired t-test; $*P < 0.05$). (D) Transwell migration assay: significantly lower migration ability was observed in TEAD4-mutated cells (unpaired t-test, $****P < 0.0001$).

Supplemental Table S1: CNVs in the Tumors from Patient 1. CNVs were analyzed in the two primary cell lines, generated from primary and relapsed tumors, and in the correspondent relapsed tumor tissue. A total of 31 amplification sites and three deletion sites were detected. Three genes including *TEAD4*, were amplified within all samples.

Fig. 1

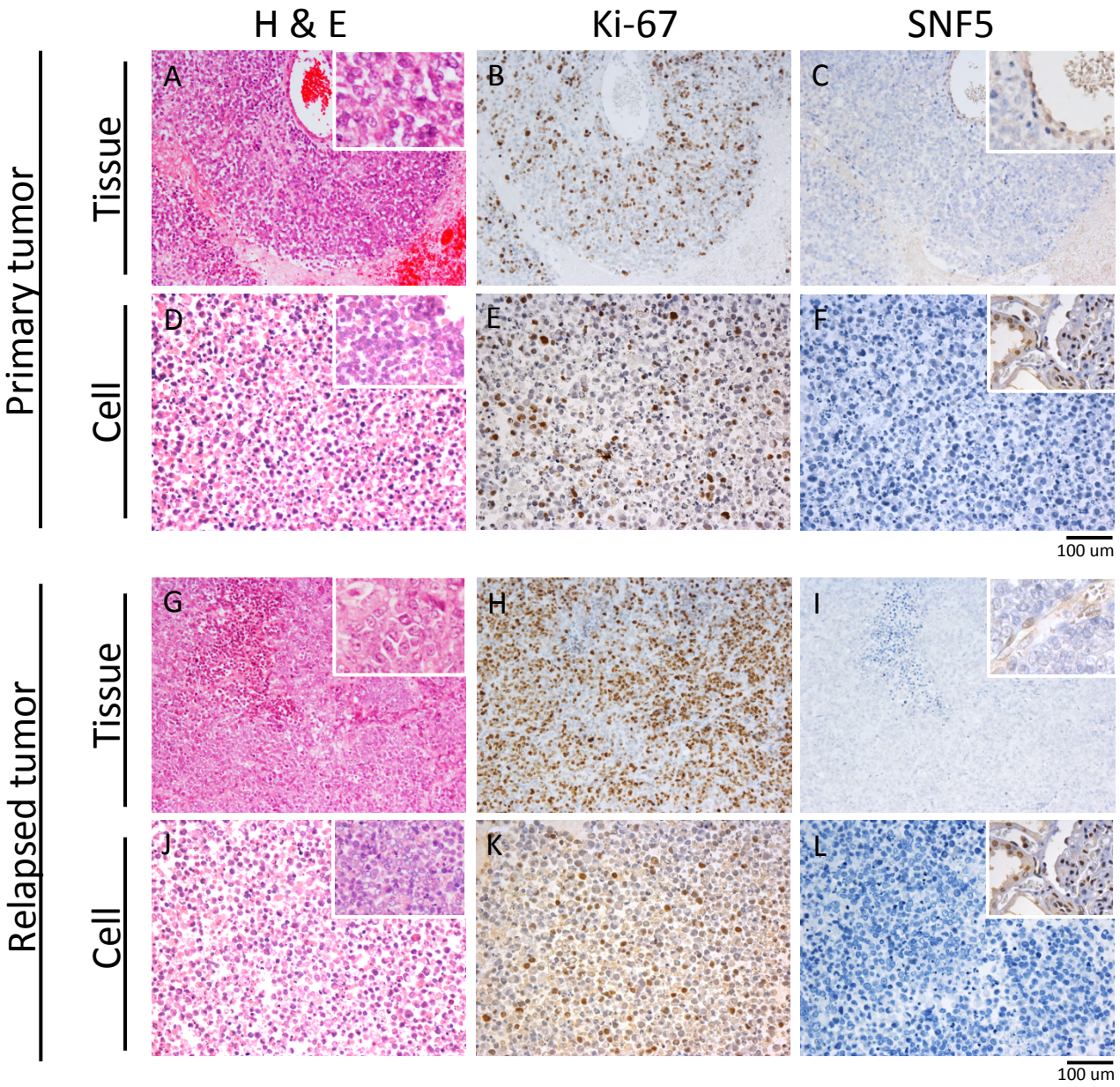
H & E
Ki-67
SNF5
Primary tumor
Tissue
Cell
Relapsed tumor
Tissue
Cell
A
B
C
D
E
F
G
H
I
J
K
L
100 um
100 um

Fig. 2

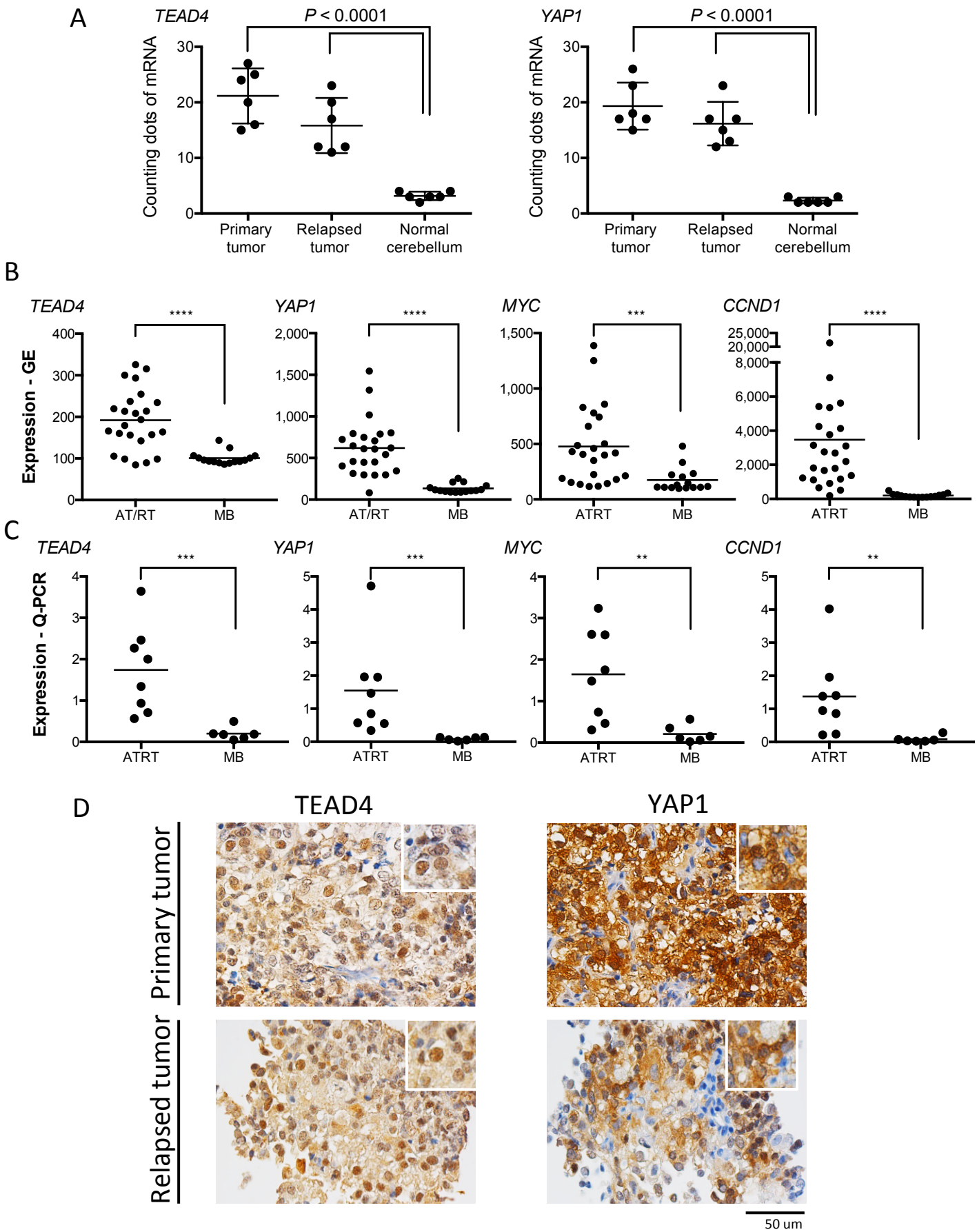
A
TEAD4
P < 0.0001
Counting dots of mRNA
30
20
10
0
Primary tumor
Relapsed tumor
Normal cerebellum
YAP1
P < 0.0001
Counting dots of mRNA
30
20
10
0
Primary tumor
Relapsed tumor
Normal cerebellum
B
TEAD4
****
YAP1
****
MYC
***
CCND1
****
Expression - GE
400
300
200
100
0
AT/RT
MB
2,000
1,500
1,000
500
0
AT/RT
MB
1,500
1,000
500
0
ATRT
MB
25,000
20,000
8,000
6,000
4,000
2,000
0
ATRT
MB
C
TEAD4
***
YAP1
***
MYC
**
CCND1
**
Expression - Q-PCR
4
3
2
1
0
ATRT
MB
5
4
3
2
1
0
ATRT
MB
4
3
2
1
0
ATRT
MB
5
4
3
2
1
0
ATRT
MB
D
TEAD4
YAP1
Primary tumor
Relapsed tumor
50 um

Fig. 3

A

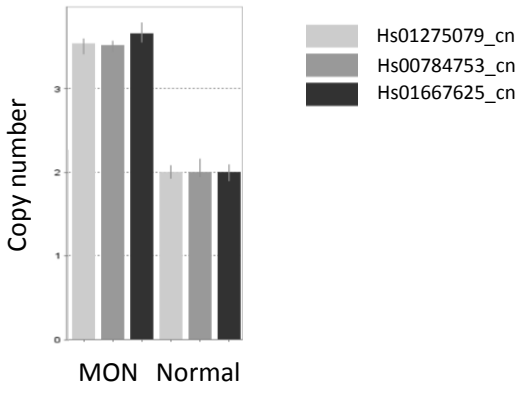
Copy number
Hs01275079_cn
Hs00784753_cn
Hs01667625_cn
MON
Normal

B

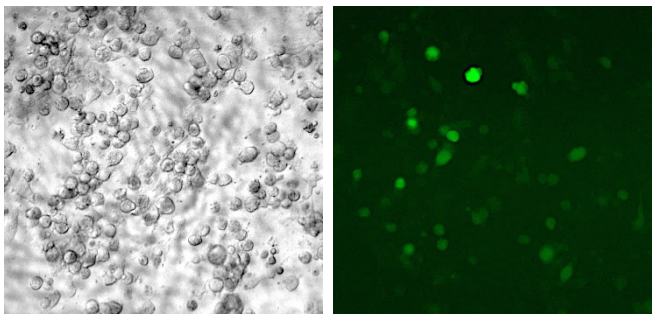

C

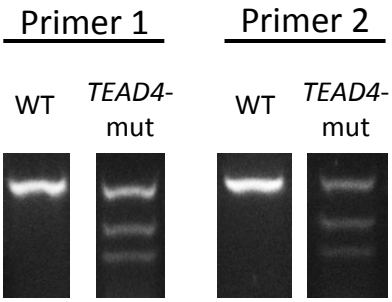
Primer 1
Primer 2
WT
TEAD4-mut
WT
TEAD4-mut

D

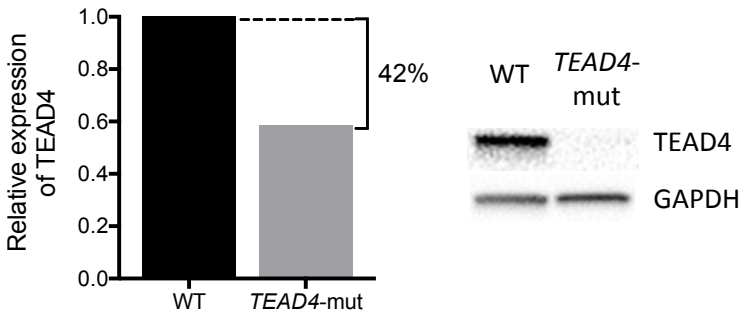
Relative expression of TEAD4
1.0
0.8
0.6
0.4
0.2
0.0
42%
WT
TEAD4-mut
WT
TEAD4-mut
TEAD4
GAPDH

Fig. 4

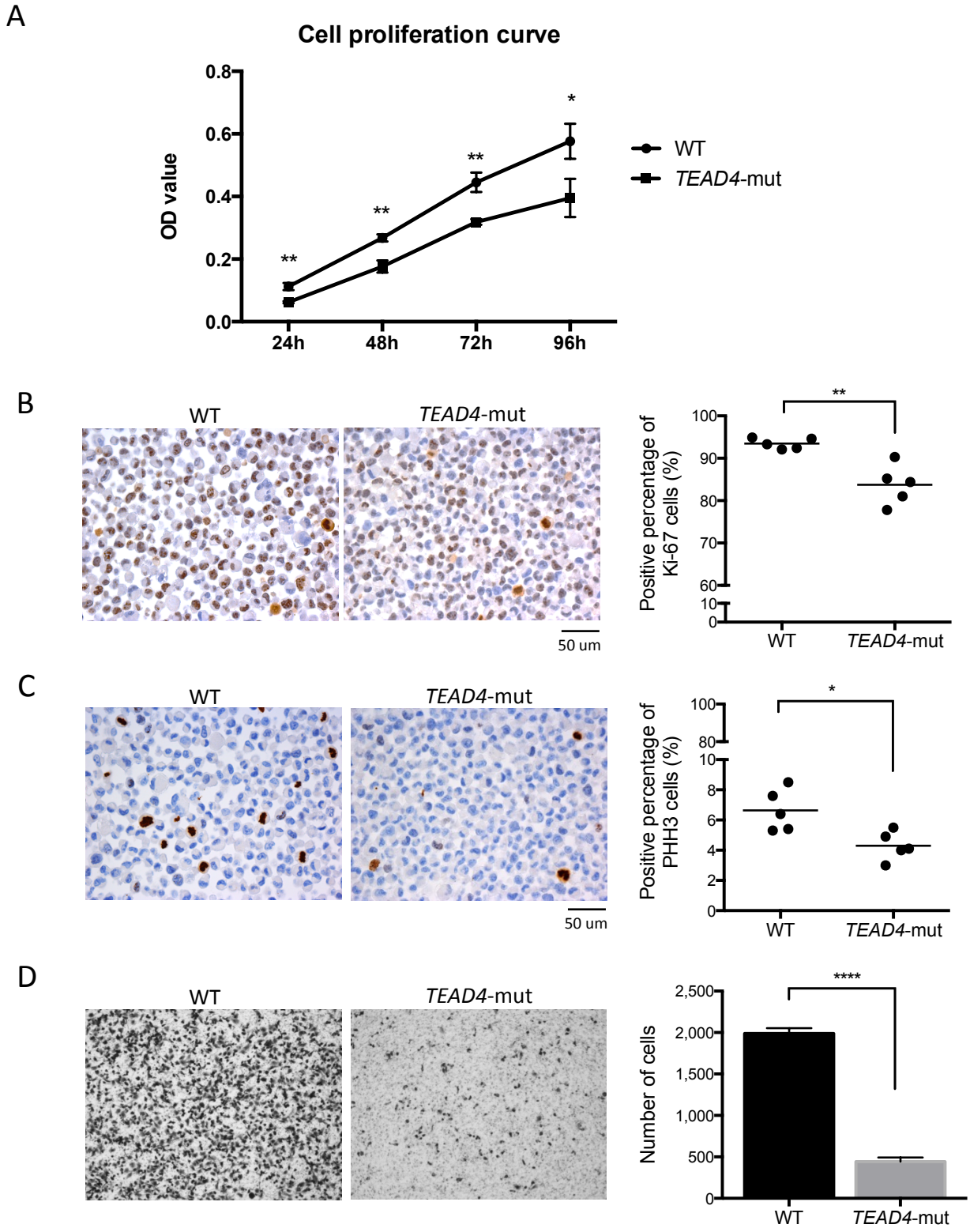
A
Cell proliferation curve
OD value
0.8
0.6
0.4
0.2
0.0
24h
48h
72h
96h
**
**
**
*
WT
TEAD4-mut
B
WT
TEAD4-mut
50 um
Positive percentage of Ki-67 cells (%)
100
90
80
70
60
10
0
**
WT
TEAD4-mut
C
WT
TEAD4-mut
50 um
Positive percentage of PHH3 cells (%)
100
80
10
8
6
4
2
0
*
WT
TEAD4-mut
D
WT
TEAD4-mut
Number of cells
2,500
2,000
1,500
1,000
500
0
****
WT
TEAD4-mut

Table 1. Summary of AT/RT Patients and Experiments

	Age	Gender	Location	Cell culture	CNV	ISH	GE/ Q-PCR	Subgroup		IHC	
								Torchia	Johann	primary	relapsed
1	6 m	F	PF	◯	◯	◯				◯	◯
2	1 y	M	PF							◯	◯
3	9 m	F	ST							◯	◯
4	1 y	F	PF							◯	
5	9m	F	PF							◯	
6	2 y	M	ST							◯	
7	13 y	M	Spine							◯	
8	3y	F	PF				◯	2	N/A	◯	
9	7 m	M	N/A				◯	2	TYR	◯	
10	4 y	M	ST				◯	1	SHH	◯	
11	6 y	M	ST				◯	2	MYC	◯	◯
12	2 m	F	PF				◯	2	TYR	◯	
13	1 y	M	ST				◯	2	N/A		
14	3 y	F	ST				◯	2	MYC		
15	11	M	ST				◯	N/A	MYC		
16	7 m	F	ST				◯	2	MYC		
17	8 m	F	ST				◯	2	MYC		
18	10 y	M	ST				◯	1	N/A		
19	N/A	N/A	ST				◯	1	SHH		
20	N/A	N/A	PF				◯	1	SHH		
21	7 m	M	PF				◯	N/A	N/A		
22	10	M	PF				◯	1	SHH		
23	1 y	M	ST				◯	N/A	SHH		
24	12 y	M	Spine				◯	2	MYC		
25	9 m	F	ST				◯	1	SHH		
26	11 y	M	N/A				◯	N/A	MYC		
27	10	M	N/A				◯	2	TYR		
28	13 y	M	Spine				◯	N/A	MYC		
29	7 m	F	ST				◯	N/A	MYC		

CNV, copy number variation; GE, gene expression; IHC, immunohistochemistry; ISH, *in situ hybridization*; m, months; N/A, not available; PF, posterior fossa Q-PCR, quantitative real-time polymerase chain reaction; ST, supra-tentorial; y, years.

Supplemental Table S1. CNVs in the Tumors from Patient 1

CN	Type	Chr	Start	Size (kbp)	Genes	Primary cell	Relapse cell	Relapse tumor tissue
0	Loss	1	q24.2	25.655	NME7		○	○
4	Gain	2	p12	14.908	CTNNA2	○		
0	Loss	3	p26.3	10.403	none	○	○	○
0	Loss	4	q13.1	10.79	none	○	○	
4	Gain	4	q32.2	70.686	none	○	○	○
4	Gain	5	q11.2	23.72	none		○	○
4	Gain	7	q35	3.106	CNTNAP2	○		
4	Gain	7	q36.1	17.491	RHEB	○	○	○
4	Gain	7	q34	69.743	TRY6, PRSS2	○		
4	Gain	7	q11.23	9.875	TYW1B	○		
4	Gain	7	p13	4.069	UBE2D4	○		
4	Gain	8	p23.1	3.19	none		○	○
4	Gain	8	p23.1	44.835	DEFA1B, DEFA1, DEFT1P, DEFT1P2, DEFA3	○		
4	Gain	8	p23.1	0.297	MFHAS1	○		
4	Gain	8	p23.1	4.058	SGK223	○		
4	Gain	9	p23	9.209	PTPRD	○		
4	Gain	10	q24.2	14.27	DNMBP, NCRNA00093	○		
4	Gain	10	q23.1	0.754	NRG3	○		
4	Gain	11	q11	56.285	none	○	○	○
4	Gain	11	p14.1	13.499	none	○		
4	Gain	12	q24.33	6.43	ANKLE2	○		
4	Gain	12	q14.3	5.385	GRIP1	○		
4	Gain	12	p13.2	16.483	KLRC2	○	○	
4	Gain	12	p13.33	24.092	TEAD4	○	○	○
4	Gain	14	q22.2	0.726	none	○		
4	Gain	14	q24.3	17.194	HEATR4, ACOT1	○		
4	Gain	14	q21.3	8.032	MDGA2	○		
4	Gain	17	q21.2	9.827	none	○		
4	Gain	17	p13.3	7.93	DOC2B	○		
4	Gain	18	q21.31	1.042	NEDD4L	○		
4	Gain	19	q13.42	10.461	LILRA3		○	○
4	Gain	20	q13.33	3.664	none	○		
4	Gain	20	p11.23	6.789	C20orf26	○		
4	Gain	21	q22.3	4.996	HSF2BP	○	○	○

Chr, chromosome; CN, copy number, CNVs, copy number variations.